Clim. Past, 13, 1007–1022, 2017
https://doi.org/10.5194/cp-13-1007-2017

Climate of the Past
Open Access
EGU

Experiments based on blue intensity for reconstructing North Pacific temperatures along the Gulf of Alaska

Rob Wilson[1,2], Rosanne D'Arrigo[2], Laia Andreu-Hayles[2], Rose Oelkers[2], Greg Wiles[2,3], Kevin Anchukaitis[4,2], and Nicole Davi[2,5]

[1]School of Earth and Environmental Sciences, University of St. Andrews, St. Andrews, UK
[2]Tree-Ring Laboratory, Lamont–Doherty Earth Observatory, Palisades, NY, USA
[3]Department of Geology, The College of Wooster, Wooster, Ohio, USA
[4]School of Geography and Development & Laboratory of Tree Ring Research, University of Arizona, Tucson, AZ, USA
[5]Department of Environmental Science, William Paterson University, New Jersey, USA

Correspondence to: Rob Wilson (rjsw@st-andrews.ac.uk)

Received: 26 February 2017 – Discussion started: 6 March 2017
Revised: 16 June 2017 – Accepted: 26 June 2017 – Published: 16 August 2017

Abstract. Ring-width (RW) records from the Gulf of Alaska (GOA) have yielded a valuable long-term perspective for North Pacific changes on decadal to longer timescales in prior studies but contain a broad winter to late summer seasonal climate response. Similar to the highly climate-sensitive maximum latewood density (MXD) proxy, the blue intensity (BI) parameter has recently been shown to correlate well with year-to-year warm-season temperatures for a number of sites at northern latitudes. Since BI records are much less labour intensive and expensive to generate than MXD, such data hold great potential value for future tree-ring studies in the GOA and other regions in mid- to high latitudes. Here we explore the potential for improving tree-ring-based reconstructions using combinations of RW- and BI-related parameters (latewood BI and delta BI) from an experimental subset of samples at eight mountain hemlock (*Tsuga mertensiana*) sites along the GOA. This is the first study for the hemlock genus using BI data. We find that using either inverted latewood BI (LWB_{inv}) or delta BI (DB) can improve the amount of explained temperature variance by > 10 % compared to RW alone, although the optimal target season shrinks to June–September, which may have implications for studying ocean–atmosphere variability in the region. One challenge in building these BI records is that resin extraction did not remove colour differences between the heartwood and sapwood; thus, long term trend biases, expressed as relatively warm temperatures in the 18th century, were noted when using the LWB_{inv} data. Using DB appeared to overcome these trend biases, resulting in a reconstruction expressing 18th–19th century temperatures ca. 0.5 °C cooler than the 20th–21st centuries. This cool period agrees well with previous dendroclimatic studies and the glacial advance record in the region. Continuing BI measurement in the GOA region must focus on sampling and measuring more trees per site (> 20) and compiling more sites to overcome site-specific factors affecting climate response and using subfossil material to extend the record. Although LWB_{inv} captures the inter-annual climate signal more strongly than DB, DB appears to better capture long-term secular trends that agree with other proxy archives in the region. Great care is needed, however, when implementing different detrending options and more experimentation is necessary to assess the utility of DB for different conifer species around the Northern Hemisphere.

1 Introduction

The climate of the Gulf of Alaska (GOA) is strongly influenced by the atmosphere–ocean variability in the North Pacific sector (e.g. the Pacific Decadal Oscillation; Mantua et al., 1997), with profound socioeconomic implications for the region (Ebbesmeyer et al., 1991). The variability in such synoptic climate phenomena is more strongly expressed in winter. Ring-width (RW) data measured from montane treeline conifer trees in the GOA region often express a broad seasonal response window (e.g. January–September, Wilson et

al., 2007; February–August, Wiles et al., 2014), which has allowed such data to provide information on cold season synoptic dynamics covering almost 2 000 years (Barclay et al., 1999; D'Arrigo et al., 2001; Wiles et al., 2004, 2014; Wilson et al., 2007).

Maximum latewood density (MXD) measurements have yielded long records of past summer temperatures for many regions in the northern mid- to high latitudes (e.g. Schweingruber, 1988; Briffa et al., 2002; Anchukaitis et al., 2013; Schneider et al., 2015), but such records do not yet exist for the GOA. MXD series are particularly desirable as such records often have stronger correlations with temperatures than RW and result in climate reconstructions with better skill and spectral fidelity (Anchukaitis et al., 2013; Esper et al., 2015; Wilson et al., 2016; Anchukaitis et al., 2017). This is partly because RW chronologies typically exhibit higher autocorrelation and lagged memory effects than MXD (Briffa et al., 2002; Anchukaitis et al., 2012), but also because RW may potentially integrate other ecological signals (e.g. disturbance and stand dynamics), which can obscure the climate signal (Rydval et al., 2015). However, only two millennial-length MXD records are currently published for all of north-western North America (Columbia Icefield, Canada, Luckman and Wilson 2005; Firth River, Alaska, Andreu-Hayles et al., 2011; Anchukaitis et al., 2013) and no MXD data have been generated to date for the entire GOA. This situation partly relates to the expensive and labour-intensive nature of MXD measurement, but also because the wood of mountain hemlock (*Tsuga mertensiana*), a dominant conifer species in the GOA, is rather brittle and does not lend itself well to standard sample preparation for MXD measurement.

To help meet the need for additional climatically sensitive density records from north-western North America, we present herein an exploration of novel blue intensity (BI) parameters measured from scanned images of tree core samples from the GOA. Minimum latewood blue intensity (LWB) has recently been shown to have strong similarities to MXD and is much cheaper and simpler to generate (McCarroll et al., 2002; Björklund et al., 2014, 2015; Rydval et al., 2014; Wilson et al., 2014, 2017). LWB is closely related to MXD as they both measure similar wood properties (combined hemicellulose, cellulose, and lignin content related to cell wall thickness), and both are well correlated with warm-season temperatures (Campbell et al., 2007; Björklund et al., 2014; Rydval et al., 2014; Wilson et al., 2014). This correspondence between BI and temperature has recently been shown to hold true for several locations and tree species, including Scots pine (*Pinus sylvestris*) in Scotland, UK (Rydval et al., 2014), and Sweden (Björklund et al., 2014, 2015); Caucasian fir (*Abies nordmanniana*) in the Northern Caucasus (Dolgova, 2016); Stone pine (*Pinus cembra*) in Austria (Wilson et al., 2017); Engelmann spruce (*Picea engelmannii*) from the Canadian Rockies, British Columbia, Canada (Wilson et al., 2014). Although BI often requires larger sample sizes than MXD to improve signal strength (Wilson et al., 2014), this is not a concern due to the low cost of the method.

The greatest limitation of LWB, however, is that any colour variation that does not represent year-to-year climate-driven cell wall thickness changes will bias the resultant raw reflectance measurements. For example, some conifer species (including Scots pine and mountain hemlock) show a clear sharp or transitional colour change from the heartwood to sapwood, which, even after resin extraction using ethanol or acetone, can still impose a systematic change in reflectance around the heartwood/sapwood transition (Rydval et al., 2014; Björklund et al., 2014, 2015). Further colour variations, often seen in dead but preserved snag or subfossil wood, can also result in systematic biases when combined with data measured from living samples (Björklund et al., 2014, 2015; Rydval et al., 2014). Björklund et al. (2014) proposed a potential solution to the heartwood–sapwood colour bias issue by effectively detrending the LWB measurements by removing the inherent common colour changes of the early wood and latewood (i.e. those related to heartwood–sapwood colour change). This is accomplished by subtracting the raw LWB value from the maximum blue reflectance value of the early wood (EWB) for each year. The resulting new parameter, delta blue intensity (hereafter referred to as DB), should theoretically be less biased by such non-climatic-related colour changes. Although Björklund et al. (2014, 2015) presented compelling results using Scots pine in Sweden, DB has not yet been tested elsewhere or on any other species.

Finally, although BI-based variables hold great promise as an alternative proxy to MXD, another potential concern is the possibility that reflectance-based measurements may not capture low-frequency information related to long-term climate changes. Wilson et al. (2014), working with Engelmann spruce from British Columbia, which does not have a visual colour difference between the heartwood and sapwood, urged caution as both the MXD and LWB parameters were sensitive to different detrending options and there was some indication that LWB could not capture as much low-frequency information as MXD. However, this observation could not be fully addressed due to the relatively short instrumental record in British Columbia.

In this paper, building upon previous RW-based research (Wilson et al., 2007; Wiles et al., 2014), we measure BI variables (EWB, LWB, and DB) from multiple sites in the GOA to evaluate (a) whether BI can improve on previous RW-only reconstructions and (b) whether meaningful low-frequency information can be gleaned from these data by exploiting the long monthly instrumental record from Sitka, Alaska, back into the mid-19th century to validate secular trends in the tree-ring (TR) data.

Table 1. Metadata information for the eight GOA sites used in the study. The sites are ordered from east to west (see Fig. 1). All principal component analyses (PCAs) and related analyses were performed on the 1792–1990 period for which there is replication of at least five series for all eight sites. Tree-ring data were detrended using a 200-year spline for these signal strength analyses. The final four columns denote the number of series needed to attain an EPS of 0.85 (Wigley et al., 1984).

Site name	Timespan	No. of series	Period $n > 5$	MSL	RW RBAR	EWB RBAR	LWB RBAR	DB RBAR	N-RW EPS	N-EWB EPS	N-LWB EPS	N-DB EPS
Juneau Mtn. (JM)	1558–1998	17	1604–1998	238.5	0.35	0.15	0.24	0.25	10.7	32.9	17.7	17.3
McGinnis (MT)	1485–1999	15	1584–1999	363.5	0.47	0.11	0.24	0.24	6.4	46.3	17.6	18.0
Son of Repeater (SR)	1713–2009	10	1792–2007	216.7	0.33	0.12	0.17	0.25	11.3	43.5	27.5	17.4
Wright Mtn. (WM)	1610–2010	17	1738–2010	234.2	0.45	0.06	0.25	0.17	6.9	84.0	17.1	27.9
Miners Well (MW)	1479–1994	13	1640–1995	324.0	0.49	0.05	0.33	0.14	5.8	120.3	11.8	36.2
Eyak Mtn., Cordova (CVV)	1573–1992	17	1672–1992	280.6	0.46	0.15	0.32	0.29	6.5	32.1	12.0	14.2
Tebenkof (TBB)	1357–1990	15	1605–1990	339.2	0.43	0.13	0.20	0.22	7.6	37.9	22.4	19.6
Ellsworth (ELG)	1636–1991	18	1750–1990	218.5	0.40	0.14	0.24	0.29	8.6	35.7	17.7	14.2
			Median	259.6	0.44	0.12	0.24	0.24	7.23	40.70	17.62	17.69

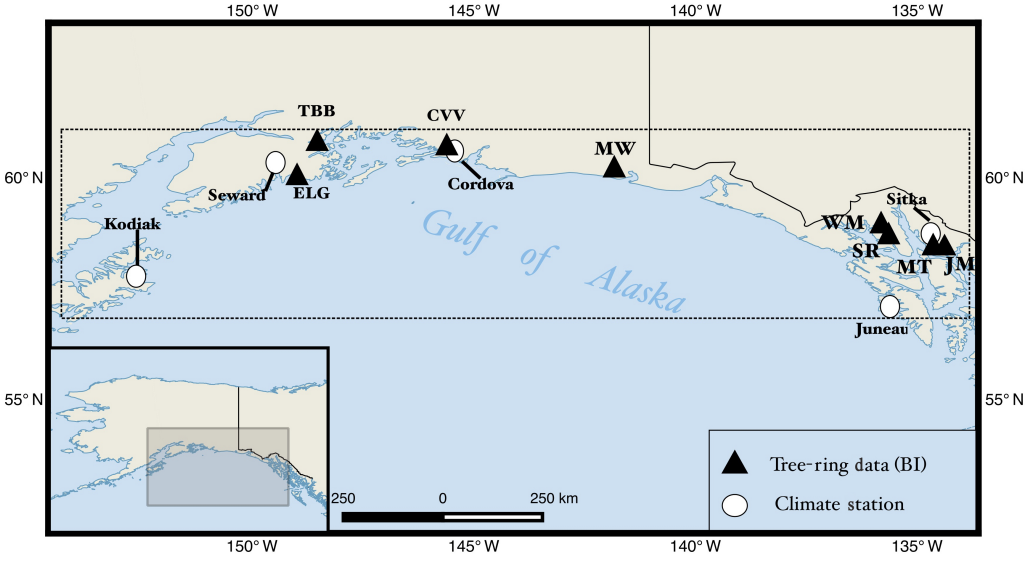

Figure 1. Location map of the eight GOA tree-ring sites used in this study (Table 1). Also indicated (dashed line box) is the domain (57–61° N, 153–134° W) of the gridded data (CRU TS 3.24, Harris et al., 2014; BEST, Rohde et al., 2012) used for calibration and the five coastal GOA temperature stations used in the original five-station mean series (Wilson et al., 2007; see Fig. S1 in the Supplement).

2 Methods and analysis

For this exploratory study, BI measurements were made on a subset (ca. 15 single tree cores per site) of cross-dated core samples collected over the past few decades from living mountain hemlock (*Tsuga mertensiana* Bong. Carrière) trees located at eight sites near altitudinal treeline (approximately ∼ 300–400 m above sea level) along the GOA (Table 1, Fig. 1). Data from these and additional sites were used previously to create coastal GOA RW-based temperature-related reconstructions (D'Arrigo et al., 2001; Wilson et al., 2007; Wiles et al., 2014).

The tree core samples were immersed in acetone for 72 h to remove excess resins in the wood (Rydval et al., 2014) and then finely sanded to 1200 grit to remove marks and abrasions prior to scanning. An Epson V850 pro scanner, using an IT8.7/2 calibration card in conjunction with SilverFast scanning software, was used to scan the samples at 2400 dpi resolution. Raw EWB and LWB variables were measured using CooRecorder 8.1 software (Cybis 2016, http://www.cybis.se/forfun/dendro/index.htm), which has the capability to acquire accurate reflectance-intensity RGB colour model measurements from scanned wood samples (see Rydval et al., 2014). DB values were calculated within CooRecorder by subtracting the raw LWB values from the raw EWB values for each year. Since raw LWB is negatively correlated with MXD (high-density dark latewood means low reflectance), values were inverted following the method detailed in Rydval et al. (2014) to allow for LWB (hereafter denoted as LWB_{inv}) to be detrended in a similar way to MXD (see also Wilson et al., 2014). The nature of the DB calculation results in this pa-

rameter being positively correlated with LWB_{inv} means that these data could also theoretically be detrended in a similar way. It should be noted that Björklund et al. (2014) proposed that LWB_{inv} should be referred to as maximum latewood blue absorption intensity.

As the mean sample length (Table 1) for all sites was > 200 years, for initial experiments comparing the different tree-ring (TR) variables, the RW, LWB_{inv}, EWB, and DB data were detrended using fixed 200-year cubic smoothing splines (Cook and Peters, 1981) to retain the interannual to multi-decadal signal and minimize any potential lower-frequency biases due to heartwood–sapwood colour changes. The variance in the site and regional composite chronologies were temporally stabilized using techniques detailed in Frank et al. (2007a). These chronology versions were assessed by (1) signal strength statistics: both common signal (via mean inter-series correlation, RBAR) and expressed population signal (EPS; Wigley et al., 1984) statistics, (2) between variable correlation, (3) between site coherence using a rotated principal component analysis (PCA, varimax rotation using correlation matrices with eigenvectors retained with an eigenvalue > 1.0), and (4) climate response derived by correlations between regional composite TR variable mean series and the dominant principal component (PC) scores against monthly and season variables of temperature (CRU TS 3.24, Harris et al., 2014: 57–61° N, 153–134° W).

The 200-year spline chronology versions were also used to explore calibration-based (1901–1960) and validation-based (1961–1989) principal component regression reconstruction experiments using the CRU TS data. The 1961–1989 period was specifically used for validation as many temperature-sensitive chronologies based on tree-ring width in Alaska do not track recent temperature trends well – a phenomenon often referred to as the "divergence problem" (D'Arrigo et al., 2008). For the PCA, a reasonably replicated common period (1792–1989) was used in which tree series replication was > 5 trees. All site chronologies are replicated with > 10 trees from 1792 except for JM and SR (see Table 1) where replication is six and five, respectively. Reconstruction validation was performed using the Pearson's correlation coefficient (r), the reduction of error (RE) and the coefficient of efficiency (CE; Cook et al., 1994). Further validation was performed over the 1850–1900 period using the gridded BEST instrumental data (Rohde et al., 2012), extracted for the same region as the CRU TS (57–61° N, 153–134° W), after these data were scaled to the CRU TS data over the 1901–2015 period. CRU TS and BEST are compared (Fig. S1 in the Supplement) to the original GOA five-station mean records used in Wilson et al. (2007) to confirm that the gridded products are good representations of the regional temperature signal. The higher variance in the pre-1950 period in the five-station mean is related to the fact that variance stabilization (Frank et al., 2007a) was not performed when this mean series was originally developed (Wilson et al., 2007) and is therefore likely a less robust measure of GOA temperatures than the gridded products.

Finally, to improve overall expressed signal strength and explore the potential of reconstructing robust low-frequency temperature changes in the region, the data from each of the eight sites were pooled to derive GOA regional composite records for each of the TR variables. These pooled composite variable datasets, with their greater overall replication, allowed detrending experiments to be performed to ascertain the sensitivity of the final parameter chronologies to different detrending choices. Specifically, RW detrending experiments were performed using (1) STD, negative exponential function or negative or zero-slope linear function detrending via division; (2) NEPT, negative exponential function or negative or zero-slope linear function detrending via subtraction after power transformation of the raw RW data (Cook and Peters, 1997); and (3) RCS, single-group regional curve standardization (Briffa et al., 1996; Esper et al., 2003; Briffa and Melvin, 2011) detrending via division. The regional age-aligned curve was smoothed using a cubic smoothing spline (Cook and Peters, 1981) of 10 % of the series length. For each of these three approaches, the signal-free (SF; Melvin and Briffa, 2008) approach to detrending was also used. Finally, the composite chronologies, also using the SF approach, were also derived using the age-dependent spline (ADS) approach introduced by Melvin et al. (2007) to track more complex growth trends that may not be captured well with the STD, NEPT, and RCS approaches. These different detrending options resulted in an ensemble of seven different RW composite chronologies. For LWB_{inv} and DB, as they should theoretically behave more like MXD, which often has a decreasing linear trend, detrending was performed using (1) LINres, negative or zero-slope linear function detrending via subtraction, with and without the SF approach; (2) RCSres, single-group RCS detrending via subtraction, with and without the SF approach; and (3) ADSsf, the signal-free age-dependent spline approach. Overall, for LWB_{inv} and DB, five chronology variants were developed for analysis.

3 Results and discussion

3.1 Common signal within the network

RW has the strongest common signal with a median overall RBAR of 0.44 (eight-site range: 0.33–0.49, Table 1), whereas LWB_{inv} and DB both have weaker RBAR values of 0.24. EWB shows the weakest common signal with a median RBAR of only 0.12 from the eight sites. In order of decreasing between-series common signal, the number of trees needed to attain an EPS of 0.85 are 7 (RW), 18 (LWB_{inv} and DB), and 41 (EWB) for each variable, respectively. On average, therefore, except for RW, actual replication for the reflectance-based parameter chronologies is often lower than would be ideally needed to attain a robust expressed population signal. This is important to keep in mind as it is likely

that the experimental calibration results presented herein will improve as replication is increased.

The weak signal strength in EWB compared to RW, LWB_{inv}, and DB is also reflected in the PCA. The leading PC for RW, LWB_{inv}, and DB explains 59, 53, and 57 % of the overall variance, respectively, while just 39 % is explained by the EWB PC1. In general, the loadings (based on a varimax rotation) of the chronologies on each PC for each variable are related to the geographical locations across the GOA, with PC1 representing the eastern sites and PC2 the western ones (Figs. 1 and 2). A similar spatial distribution of loadings was noted in Wilson et al. (2007) using RW data from 31 living sites across the GOA.

3.2 Seasonal temperature sensitivity

EWB contains a weak response to summer temperature variability with almost no late summer temperature signal (Fig. 2) although some significant correlations ($r = \sim 0.3$–0.4) are found with May and previous October–November temperatures (Fig. S2 in the Supplement). Correlations with seasonal temperatures, after first differencing, identifies no significant response (Fig. S3 in the Supplement). In agreement with previous work (Wilson et al., 2007; Wiles et al., 2014), RW correlates well with a broad range of summer seasons (Fig. 2), showing positive correlations for nearly all months from January through to September (Fig. S2 in the Supplement) with June returning the strongest correlation. Correlations do weaken when the data are first differenced (Fig. S3 in the Supplement), but the Wiles et al. (2014) RW composite still retains a strong response with February–August temperatures, although for the other RW-based time series, the summer season shows the strongest coherence. LWB_{inv} and DB show a weaker response with the late winter–spring months compared to RW and the strongest correlations with June, July, and August (Fig. 2). These observations were expected as LWB_{inv} and DB should express similar growth–climate response properties to MXD.

For the RW, LWB_{inv}, and DB data, there appears to be a geographical difference in response, with PC1 (eastern sites) showing stronger seasonal (Fig. 2) and monthly (Fig. S2 in the Supplement) correlations with temperature than PC2 (western sites). However, correlations between the individual site chronologies for each TR variable (Table 2) and June–September temperatures (optimal season for reconstruction – see later) suggest that there is a degree of variability in the individual sites' response to summer temperatures across the GOA. As PC2 is weighted more towards the TBB site (see PCA loadings in Fig. 2 for RW, LWB_{inv}, and DB), which correlates weakly with JJAS, it is therefore not surprising that this PC correlates weakly with summer temperatures. After first differencing, however, these regional differences disappear (Fig. S3 in the Supplement), suggesting that there are potential post-detrending trend biases in the chronologies weighted on PC2.

It is important to note that the correlation of the mean composite chronologies with summer temperatures (Fig. 2 and especially Fig. S3 in the Supplement after a first differenced transformation) are stronger than the PC1 results. This suggests that a regional mean composite approach is potentially optimal in the context of deriving a GOA-wide reconstruction, which can be extended in the future by data generated from subfossil samples.

The positive correlation of RW, LWB_{inv}, and DB with summer temperatures (Fig. 2 and Table 2) is also reflected in the intercorrelation between these different variables (Table 3). RW agrees most strongly with DB, followed by LWB_{inv}. EWB, unsurprisingly, has the weakest relationship with the other three TR variables. Hereafter, due to the poor signal strength and weak climate signal, the EWB data were not used for further analysis, except in the DB calculations.

3.3 Calibration–validation experiments

Calibration and validation statistics for various PC regression variable combinations for several summer target seasons are detailed in Table 4 along with results using the GOA RW composite of Wiles et al. (2014). Firstly, calibration of Wiles et al. (2014) to the CRU TS 3.24 data (February–August) over the 1901–1989 period ($r^2 = 0.33$) is stronger than the new RW GOA composite ($r^2 = 0.27$), which also shows a significant trend in the model residuals. This residual trend possibly reflects the fact that there could be a longer-term trend missing in the RW data due to the use of 200-year spline detrended chronologies when compared to the RCS processed version of Wiles et al. (2014). Also, the slightly weaker results for the new RW data likely reflect lower replication in the current study compared to Wiles et al. (2014).

The strongest calibration ${}_a r^2$ values for each BI parameter over the 1901–1960 period are 0.49 and 0.47 for LWB_{inv} and DB, respectively, for the JJA season, although DB fails validation with negative RE and CE values over the 1961–1989 period. Minimal model improvement is gained by including RW data. RW + LWB_{inv} calibrates best (${}_a r^2 = 0.49$) with JJA, while RW + DB explains more temperature variance for MJJAS (${}_a r^2 = 0.51$). However, in both cases, validation RE and CE are negative. Focussing on the full period (1901–1989) calibration, the strongest results are found for the JJAS season for all parameter options, with ${}_a r^2$ values of 0.27 (RW), 0.43 (LWB_{inv}), 0.38 (DB), 0.38 (RW + LWB_{inv}), and 0.39 (RW + DB) with no first-order autocorrelation observed for any version. Importantly, only the RW + DB version shows no significant linear trend in the model residuals. The full period (1901–1989) calibrated reconstructions (Table 4) for each of the variable options are presented in Fig. 3 along with independent validation (1850–1900) with the BEST gridded data. All parameter iterations fail validation (negative CE values) except for RW + DB, which returns positive RE (0.57) and CE (0.19) values. Overall, using this subset of samples from these eight sites, the calibra-

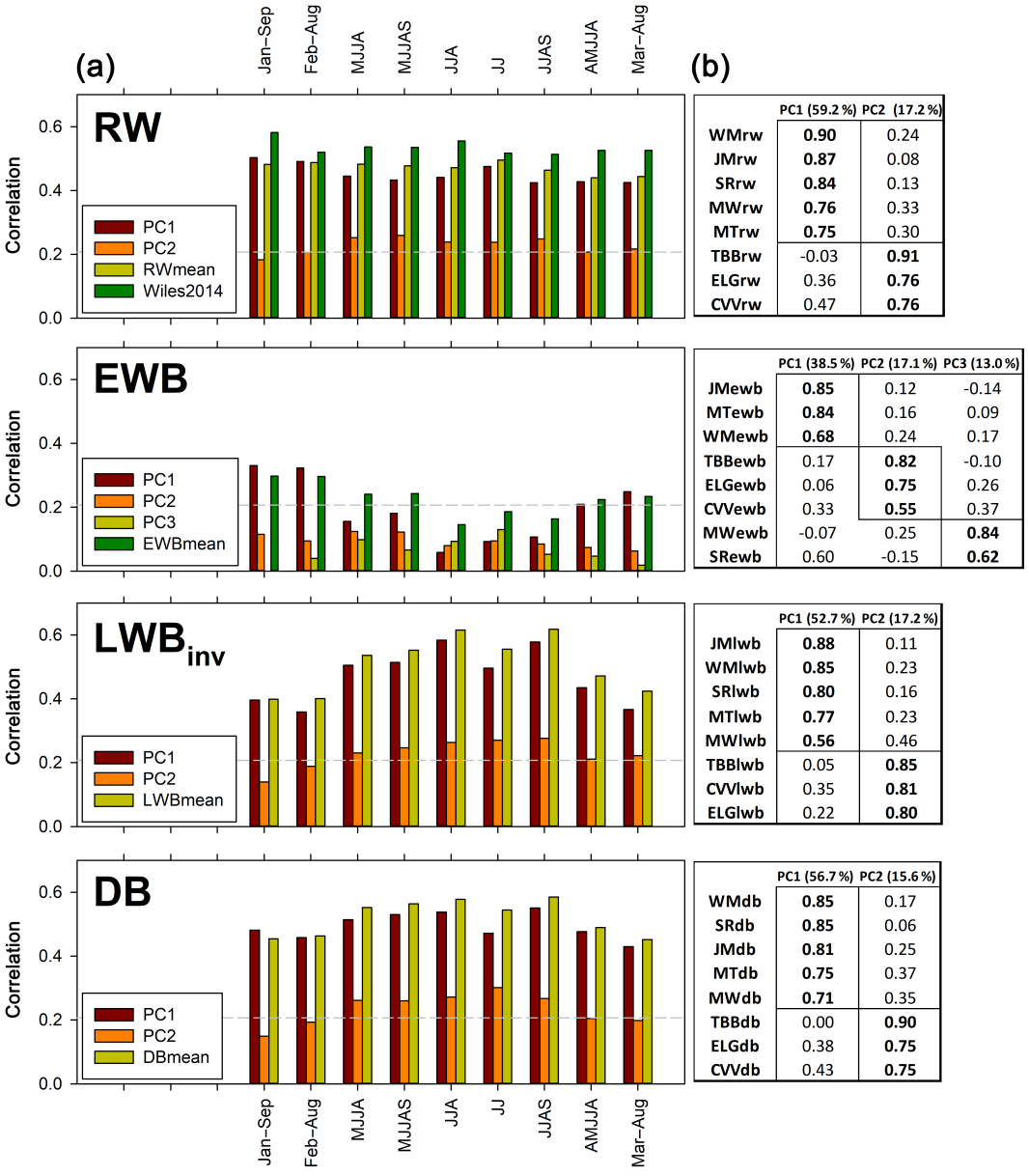

Figure 2. **(a)** Correlation response function analysis (1901–1989) using CRU TS 3.24 mean temperatures with each tree-ring variable (RW: ring width; EWB: early wood maximum blue intensity; LWB_{inv}: inverted latewood minimum blue intensity; DB: delta blue). The bars represent correlations with seasonal temperature for each principal component (PC) score and the simple GOA mean composite. Also for RW, correlations are shown for the Wiles et al. (2014) RW-based RCS reconstruction. Horizontal line denotes the 95 % confidence limit. Correlations with individual months are presented in Fig. S2 in the Supplement. **(b)** Varimax rotation principal component analysis results showing loadings of each chronology on each PC with an eigenvalue > 1.0. % denote the explained amount of variance of the original data input matrix each PC explains.

tion results (Table 4 and Fig. 3) indicate that BI-based parameters explain more temperature variance than using RW alone. However, the fidelity of the resultant reconstructions appears sensitive to the periods of calibration and validation used and it is not clear which of these parameters best represents longer-term secular change as the chronologies were limited in the frequency domain by using a fixed 200-year spline detrending option.

The large-scale climate signal expressed by these data is illustrated by comparing the RW+DB JJAS reconstruction with gridded land and sea HadCRUT4 (Morice et al., 2012; Cowtan and Way, 2014 – Fig. 4a) and land-only CRU TS 3.24 (Harris et al., 2014 – Fig. 4b) temperatures for the GOA and

Table 2. Correlations (1850–1900, 1901–1990, and 1850–1990) for each site RW, LWB_{inv}, and DB chronology with JJAS temperatures. EWB correlations are not shown. The sites are ordered from east to west (see Fig. 1).

RW	JM	MT	SR	WM	MW	CVV	TBB	ELG
1850–1900	0.45	0.22	0.49	0.22	0.27	0.30	0.30	0.38
1901–1990	0.49	0.26	0.42	0.41	0.36	0.41	0.20	0.34
1850–1990	0.50	0.37	0.47	0.43	0.39	0.47	0.33	0.39
LWB_{inv}	JM	MT	SR	WM	MW	CVV	TBB	ELG
1850–1900	0.45	0.29	0.48	0.38	0.49	0.40	0.25	0.46
1901–1990	0.52	0.39	0.64	0.58	0.46	0.45	0.28	0.41
1850–1990	0.37	0.32	0.55	0.46	0.53	0.51	0.33	0.44
DB	JM	MT	SR	WM	MW	CVV	TBB	ELG
1850–1900	0.45	0.29	0.49	0.23	0.35	0.40	0.37	0.48
1901–1990	0.57	0.45	0.58	0.47	0.48	0.50	0.23	0.39
1850–1990	0.53	0.44	0.48	0.38	0.44	0.52	0.34	0.44

Table 3. Correlation matrix between the different tree-ring variable chronologies (200-year spline detrended). These values represent the averages for between TR variable correlations performed separately for each site.

Mean *r*	RW	EWB	LWB	DB
RW		0.27	0.68	0.81
EWB			−0.23	0.36
LWB				0.80
DB				

North Pacific sectors. Although the spatial correlations are stronger towards Juneau and Sitka (see Fig. 1 for locations) in the east of the region, it is clear that these new data represent the temperature variability in the wider GOA region and North Pacific. Continued measurement of BI-based parameters from subfossil samples taken from across the GOA will allow long-term summer temperature variability to be derived for at least the last millennium, which will complement the long RW-based temperature reconstructions expressing a broader seasonal window (Wilson et al., 2007; Wiles et al., 2014).

3.4 Potential low-frequency bias

The main potential limitation to the use of BI-based TR variables such as LWB is concerned with low-frequency trend biases related to wood colour change. Mountain hemlock, in general, shows darker heartwood and lighter sapwood, which resin extraction appears to only minimize but not entirely remove. However, this colour change is not a sharp transition and is expressed in raw EWB and LWB measurements as a steady increase in reflectance intensity. Non-detrended mean composite chronologies of EWB and LWB for the whole GOA region (Fig. 5) clearly show the impact of the heartwood–sapwood colour change with increasing intensity values through time (see also Fig. S4 in the Supplement for a single tree example), especially since the late 18th century. In contrast, MXD generally shows a linear decreasing trend with increasing cambial age (Esper et al., 2012). If LWB is indeed a comparable (but inverted) TR variable to MXD as a measure of latewood anatomical density properties, then we would therefore expect an increasing trend in raw LWB values. Figure 5 therefore poses a potential mixed-signal conundrum as the observed trend in the GOA raw mean LWB composite will incorporate the secular climate signal, the true age-related trend in changing latewood density, and the heartwood–sapwood colour change bias. Although using DB can theoretically overcome the colour bias issue, it has not been explored in any detail beyond the original concept papers (Björklund et al., 2014, 2015). The mean DB non-detrended GOA chronology (Fig. 5) has minimal long-term trends, which could suggest that the colour change bias has been removed or at least minimized.

Mean cambial age-aligned curves of the EWB, LWB, and DB data show very distinct trends (Fig. S5 in the Supplement). LWB appears to show a general linear increase in values – a trend that would be expected if LWB does indeed reflect similar wood properties (inversely) to MXD. DB, however, has a more complex mean growth curve, essentially reflecting trends in the EWB data, and shows an initial increasing juvenile trend for ∼ 50 years, a period of stabilization and then a decreasing trend from about ∼ 200 to 300 years. These different age-aligned curves highlight that different detrending options may well be needed for these different TR variables.

A range of credible options for detrending the RW, LWB_{inv}, and DB GOA regional composite data are presented in Fig. 6. The outcome for the RW data appears extremely consistent even when using STD- vs. RCS-based methods. However, the LWB_{inv} and DB chronologies are much more

Table 4. Calibration experiments for the four strongest seasons (see Fig. 2). Initial calibration (using CRU TS 3.24) was made over 1901–1960 and validation over 1961–1989. Full calibration (1901–1989) was also performed to allow for residual tests and extra validation using BEST (1850–1990; see Fig. 2). Results in bold font do not pass significance. r: Pearson's correlation coefficient; r^2: coefficient of determination; ${}_a r^2$: r^2 adjusted for the number of predictors in the model; RE: reduction of error; CE: coefficient of efficiency; DW: Durbin–Watson test for residual autocorrelation; LINr: linear trend in the residuals.

		1901–1960 calibration			1961–1989 validation			1901–1989 full calibration + residuals			
Wiles14	Season	Series entered	r	r^2	r	RE	CE	r	r^2	DW	Linr
	MJJA	Wiles2014	0.60	0.36	0.48	0.11	0.10	0.55	0.30	1.62	0.15
	MJJAS	Wiles2014	0.55	0.30	0.53	0.21	0.20	0.53	0.28	1.72	0.17
	JJA	Wiles2014	0.58	0.34	0.47	0.06	0.05	0.53	0.28	1.75	0.17
	JJAS	Wiles2014	0.52	0.27	0.53	0.20	0.20	0.51	0.26	1.77	0.18
	Feb–Aug	Wiles2014	0.60	0.36	0.54	0.23	0.23	0.57	0.33	1.78	0.17
RW	Season	PCs entered	r	${}_a r^2$	r	RE	CE	r	${}_a r^2$	DW	Linr
	MJJA	1, 2	0.60	0.34	0.40	0.03	0.03	0.52	0.26	1.60	**0.21**
	MJJAS	1, 2	0.56	0.29	0.46	0.15	0.14	0.52	0.25	1.70	**0.23**
	JJA	1, 2	0.58	0.31	0.42	**−0.01**	**−0.02**	0.51	0.24	1.74	**0.23**
	JJAS	2, 1	0.53	0.26	0.49	0.16	0.15	0.51	0.24	1.76	**0.24**
	Feb–Aug	2, 1	0.60	0.36	0.46	0.08	0.08	0.54	0.27	1.75	**0.23**
LWB_{inv}	Season	PCs entered	r	${}_a r^2$	r	RE	CE	r	${}_a r^2$	DW	Linr
	MJJA	1, 2	0.63	0.38	0.49	0.15	0.14	0.57	0.31	**1.39**	0.20
	MJJAS	1, 2	0.63	0.37	0.55	0.23	0.22	0.59	0.34	1.50	**0.23**
	JJA	1, 2	0.71	0.49	0.58	0.16	0.15	0.66	0.42	**1.45**	**0.25**
	JJAS	1, 2	0.69	0.46	0.64	0.27	0.27	0.66	0.43	1.51	**0.27**
DB	Season	PCs entered	r	${}_a r^2$	r	RE	CE	r	${}_a r^2$	DW	Linr
	MJJA	1, 2	0.69	0.45	0.43	**−0.01**	**−0.02**	0.59	0.33	1.55	**0.24**
	MJJAS	1, 2	0.67	0.43	0.50	0.09	0.08	0.61	0.37	1.68	**0.26**
	JJA	1, 2	0.70	0.47	0.50	**−0.05**	**−0.05**	0.62	0.36	1.65	**0.26**
	JJAS	1, 2	0.68	0.44	0.58	0.11	0.11	0.63	0.38	1.72	**0.29**
RW +,LWB_{inv}	Season	PCs entered	r	${}_a r^2$	r	RE	CE	r	${}_a r^2$	DW	Linr
	MJJA	1, 2	0.69	0.45	0.46	0.03	0.03	0.60	0.34	1.67	0.18
	MJJAS	1, 2	0.66	0.43	0.51	0.13	0.12	0.62	0.37	1.87	0.20
	JJA	1, 2, 3	0.72	0.49	0.52	**−0.07**	**−0.08**	0.63	0.37	1.56	**0.26**
	JJAS	1, 2, 3	0.68	0.43	0.59	0.12	0.12	0.63	0.38	1.63	**0.28**
RW + DB	Season	PCs entered	r	${}_a r^2$	r	RE	CE	r	${}_a r^2$	DW	Linr
	MJJA	1, 2	0.71	0.49	0.44	**−0.16**	**−0.16**	0.62	0.36	1.69	0.04
	MJJAS	1, 2	0.72	0.51	0.49	**−0.14**	**−0.15**	0.61	0.36	1.78	−0.11
	JJA	1, 2, 3	0.72	0.50	0.49	**−0.15**	**−0.15**	0.56	0.32	1.89	−0.12
	JJAS	1, 2	0.71	0.49	0.52	**−0.18**	**−0.18**	0.64	0.39	1.84	0.05

sensitive to the detrending method used. Compared to RW and DB, all LWB_{inv} chronology variants show above-zero index values in the 18th century, which likely reflects the low reflectance bias of the darker heartwood compared to the sapwood because the LWB_{inv} data have been inverted. The RCS versions appear particularly inflated and as LWB_{inv} is positively correlated with summer temperatures (Fig. 2), this would result in markedly warm temperature estimates during the Little Ice Age (LIA) compared to the 20th century, which is at odds with previous GOA dendroclimatic analyses (Wiles et al., 2014) and the geomorphological record, which indicate substantial cool conditions and glacial advance from the 17th to 19th centuries (Wiles et al., 2004; Solomina et al., 2016). RCS can impart significant low-frequency bias when the assumptions and requirements of the method are not met (Melvin and Briffa, 2014; Anchukaitis et al., 2013). Furthermore, as the GOA composite utilizes only living trees, this is a far from optimal sample design for this detrending

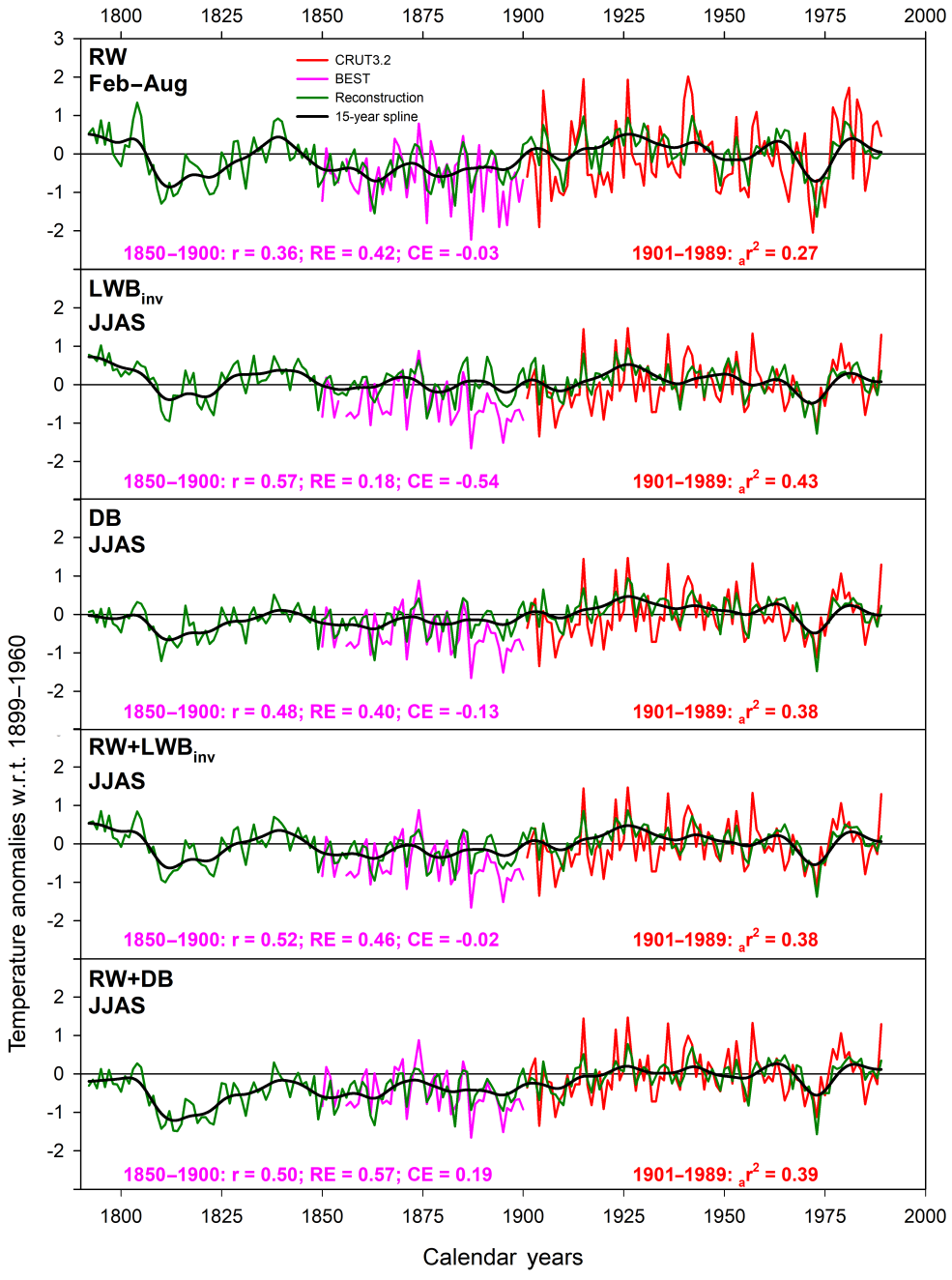

Figure 3. Illustration of the various PC regression experiments performed herein, with each reconstruction model compared with June–September (Table 3). February–August is shown for RW as that was the reconstructed season in Wiles et al. (2014). Full period calibration is performed on the 1901–1989 period (Table 3 – CRU TS 3.24) while validation (Pearson's correlation coefficient, r; reduction of error, RE; and coefficient of efficiency, CE) is undertaken over 1850–1900 using the BEST gridded data after those data were scaled to the CRU TS 3.24 data over the 1901–1989 period.

method. For DB, the LINsf version deviates markedly from LINres, RCSres, RCSsf, and ADSsf variants with very low values (< -6 standard deviation from 1901–1989 mean) before 1700 followed by a strong linear increase until present. A similar observation was noted in Wilson et al. (2014) in which signal-free detrending of LWB$_{inv}$ and MXD resulted in much cooler LIA conditions than other detrending approaches.

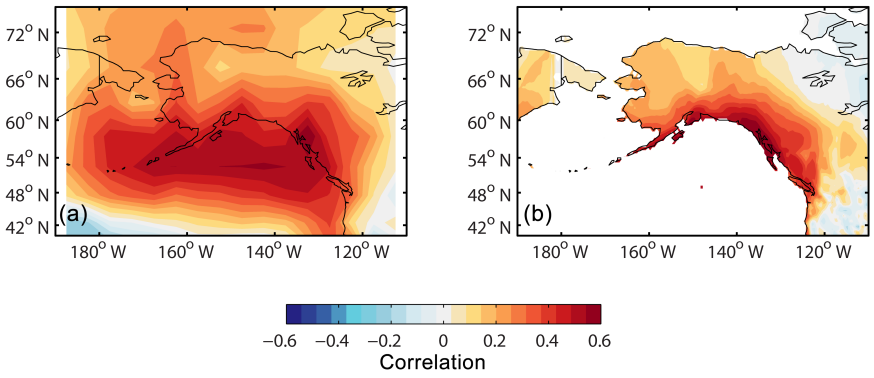

Figure 4. Spatial correlation (1901–1989) fields comparing the RW+DB GOA JJAS temperature reconstruction with larger-scale temperatures. **(a)** HADCRUT4 land and sea surface temperature (Morice et al., 2012; Cowtan and Way, 2014); **(b)** CRU TS 3.24 land temperatures (Harris et al., 2014).

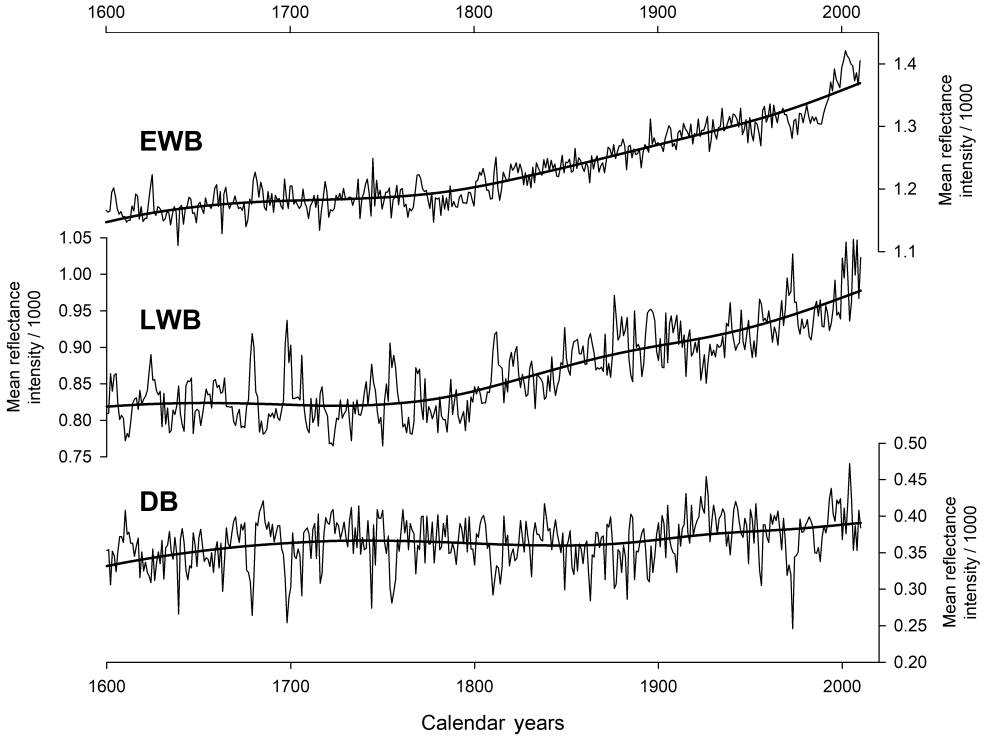

Figure 5. Mean non-detrended GOA-wide composite chronologies since 1600 for EWB, LWB (non-inverted), and DB. The LWB data have not been inverted for this figure.

3.5 JJAS GOA summer temperatures back to 1600

The long GOA instrumental record allows for additional assessment of how different reflectance-based chronology variants track temperatures back through time. Using the extended BI-based regional composite records, further reconstruction experiments against the JJAS season were performed using LWB_{inv} and DB separately (Table 5) by calibrating against JJAS CRU TS 3.24 (1901–2010) and separately validating using the BEST data (1850–1900). For the LWB_{inv} data, due to their strong post-1970s decreasing trends (Fig. 6), RCSres and RCSsf calibrated poorly (Table 5: $r^2 = 0.07$ and 0.05, respectively) and were validated with negative CE values over the 1850–1900 period. LINres and LINsf explained 41 % of the temperature variance, while the ADSsf variant explained 47 %. All three versions validated reasonably well with positive RE and CE values. Significant first-order autocorrelation (DW range 1.28 to 1.37) and linear trends (LINr range 0.36 to 0.48) were however noted for all model residuals except for ADSsf. For the DB data, calibration was strongest for RCSsf, RCSres, and ADSsf, with pos-

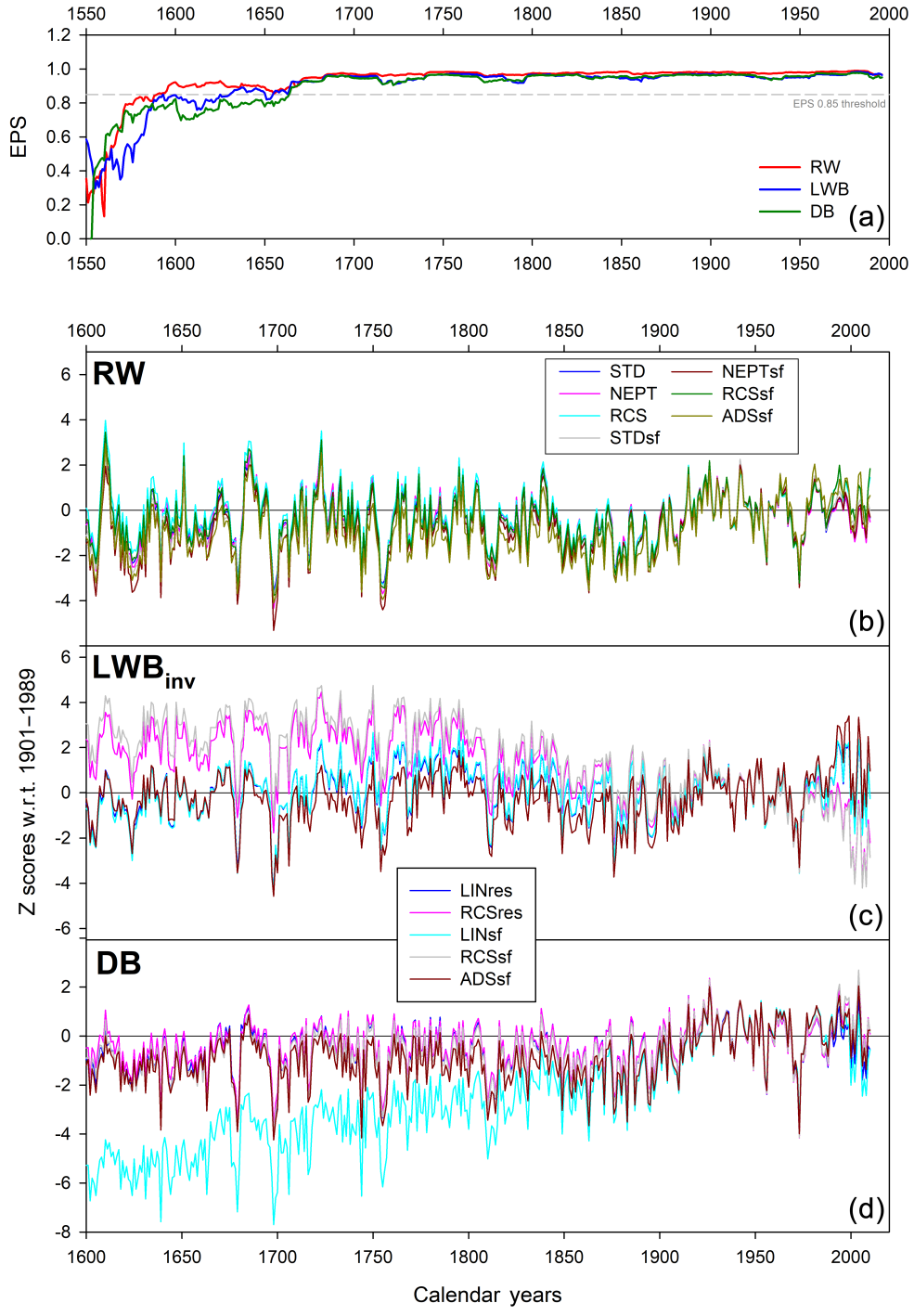

Figure 6. Detrending experiments for each TR variable using the full GOA regional composite (data from all eight sites). Panel **(a)** shows 31-year moving EPS plots for RW, LWB_{inv}, and DB using 200-year spline detrending. Panels **(b, c, d)** present chronology variants from 1600 to 2010. RW – STD: negative exponential detrending (ratio) or regression function of zero or negative slope; NEPT: as STD but raw data have been power transformed and detrended via subtraction; RCS: single-group RCS detrending (ratio); STDsf, NEPTsf, and RCSsf: as previous three options but using signal-free detrending; ADSsf: age-dependent spline detrending using signal-free detrending. For LWB_{inv} and DB – LINres: detrending via subtraction using linear functions (negative or zero slope); RCSres: as RCS above but detrending via subtraction; LINsf and RCSsf: as with LINres and RCSres but with signal-free detrending; ADSsf: age-dependent spline detrending using signal-free detrending.

Table 5. Extended reconstruction calibration experiments using different chronology versions (Fig. 6) of LWB_{inv} and DB. Results in bold font do not pass significance.

		1901–2010 calibration				1850–1900 validation		
	Series entered	r	r^2	DW	LINr	r	RE	CE
LWB_{inv}	LINres	0.64	0.41	**1.36**	**0.36**	0.53	0.44	0.07
	RCSres	0.26	0.07	**1.28**	**0.48**	0.56	0.01	**−0.64**
	LINsf	0.64	0.41	**1.37**	**0.36**	0.53	0.43	0.06
	RCSsf	0.21	0.05	**1.32**	**0.46**	0.56	**−0.05**	**−0.73**
	ADSsf	0.69	0.47	1.58	0.06	0.50	0.51	0.20
		1901–2010 calibration				1850–1900 validation		
	Series entered	r	r^2	DW	LINr	r	RE	CE
DB	LINres	0.55	0.31	**1.37**	**0.50**	0.50	0.52	0.21
	RCSres	0.64	0.40	1.59	**0.40**	0.48	0.50	0.18
	LINSF	0.54	0.29	**1.35**	**0.38**	0.43	0.40	0.00
	RCSsf	0.65	0.43	1.64	**0.35**	0.47	0.48	0.15
	ADSsf	0.65	0.42	1.59	**0.30**	0.47	0.34	**−0.09**

itive RE and CE values for all versions except ADSsf, which failed the CE test. The residuals from the RCSsf, RCSres, and ADSsf calibrations show no first-order autocorrelation although a significant linear trend is observed.

Considering the calibration and validation experiments presented in Tables 4 and 5, our results do not definitively identify whether LWB_{inv} or DB is the optimal BI-based parameter for reconstructing past summer temperatures for the GOA region. Part of this ambiguity potentially stems from unknown uncertainties in the 19th century instrumental data, but the sensitivity of the TR parameters to different detrending options (Fig. 6) exacerbates the situation. Calibration suggests that the inter-annually based signal of LWB_{inv} is marginally stronger than DB, but validation against the 19th century data cannot distinguish between the different parameters. The clear differences between the chronology versions (Fig. 6), especially before 1850, have huge implications for understanding past temperatures in the region.

To try and derive a parameter-specific view of long-term temperature changes for the region, a weighted mean using the five different variants was combined to create a regional average. The r^2 values, derived from the 1901–2010 calibration (Table 5), was used as a weighting term to calculate the parameter-specific weighted averages, which were then calibrated (1901–2010) and validated (1850–1900) in the same way as detailed in Table 5. The resultant weighted LWB_{inv} and DB regional reconstructions report quite different histories of past GOA temperatures (Fig. 7). Specifically, the LWB_{inv} reconstruction has temperature estimates from the late 17th to mid-19th century warmer than the 1961–1990 mean, while the DB reconstructions exhibit generally cooler conditions. Both reconstructions explain a similar amount of summer temperature variance (LWB_{inv}: 43 % vs. DB: 40 %) and validate with positive RE and CE values well. The regression residuals from both versions have a significant linear trend, but only for DB was no significant first-order autocorrelation identified in the residuals. Therefore, from comparison to the instrumental data alone, one cannot objectively identify which of the two parameter versions is most robust. Wilson et al. (2014) highlighted the difficulties of relying solely on the instrumental data to validate the long-term trend in any reconstruction. Moreover, there could be unknown inhomogeneity issues in early instrumental data series that are difficult to identify, which would influence calibration and validation (see Frank et al., 2007b). Therefore, alternative sources of relevant information are recommended for further validation. As the geomorphological record in the region suggests that a prolonged period of glacial advance occurred in the GOA up to the early 20th century (Wiles et al., 2004; Solomina et al., 2016) when a substantial retreat started, we hypothesize that the pre-1900 period must have therefore been cooler. This would suggest that the DB-based reconstruction is likely more representative of past GOA temperatures than the LWB_{inv}-driven one.

Figure 8 presents the RW + DB principal component reconstruction (Fig. 3), the weighted LWB_{inv} and DB extended reconstructions (Fig. 6), and the Wiles et al. (2014) RW-based reconstruction and compares them to the GOA regional glacial advance record (Wiles et al., 2004; Solomina et al., 2016). The LWB_{inv} reconstruction is clearly at odds with the other records, with temperatures that are warmer than average for many periods over the last 400 years and no specific prolonged cooler periods through the LIA. The other TR reconstructions demonstrate centennial and multi-decadal agreement, although the extended DB reconstruction exhibits a smaller amplitude of temperature change between the LIA period and the 20th century. Overall, temperatures in the GOA region were below the 1961–1990 norm through-

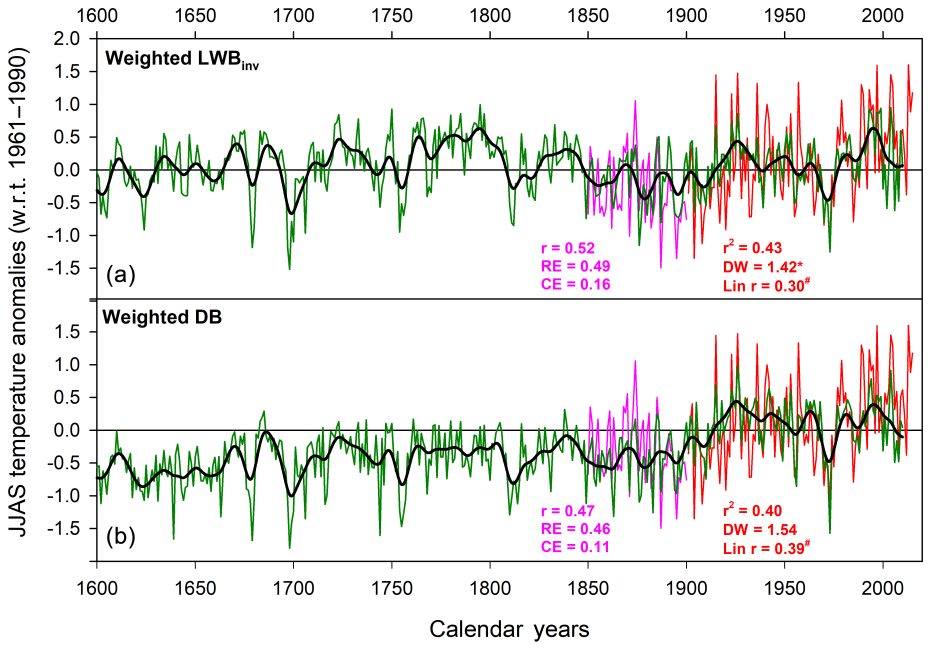

Figure 7. Extended reconstruction tests using LWB_{inv} and DB regional weighted averages. The 1901–2010 period calibration uses CRU TS 3.24 data (red) while validation is performed using BEST data (pink) over the 1850–1900 period. * denotes significant first-order autocorrelation in model residuals; # denotes a significant linear trend in the model residuals. The smoothed functions are 15-year cubic smoothing splines.

out most of the LIA, with temperatures only rising to substantially higher values in the early 20th century. The coldest decadal periods are centred around the 1700s, 1750s, and 1810s. The glacial advance record shows periods of advance through the LIA, peaking at the end of the 19th century. Despite the use of 200-year spline detrended chronologies, the RW + DB reconstruction has a similar amplitude change to the Wiles et al. (2014) record, which was derived from RCS-processed RW data. It should be also noted that this RW-based reconstruction was calibrated against February–August temperatures, which have a greater increasing temperature trend (0.81 °C increase per century vs. 0.62 °C increase per century) and higher variance (0.79 vs. 0.41) than JJAS (calculated using BEST data from 1850 to 2015), which will influence the amplitude of the reconstruction (Esper et al., 2005).

4 Conclusions

We have described a set of experimental temperature reconstructions based on RW, LWB_{inv}, and DB data measured from eight tree-ring sites along the Gulf of Alaska. Focussing on these data sets, the results demonstrate that inclusion of BI-based variables can significantly improve the calibrated variance explained using RW alone by more than 10 %.

RW, LWB_{inv}, and DB are strongly correlated with each other (Table 3) but the inclusion of LWB_{inv} or DB shifts the calibrated signal from a broad (February–August; Wiles et al., 2014) season using RW alone to a late summer (JJAS) season. The influence of late winter and early spring temperatures on RW suggest that this variable may, in fact, still be the more optimal variable for studying important synoptic phenomena such as North Pacific variability, which dominates in the winter months (Wilson et al., 2007).

The LWB_{inv} data, for mountain hemlock, despite calibrating and validating in a similar way to DB, are clearly affected by heartwood–sapwood colour differences, which impart a trend bias in the resultant chronologies and reconstructions (Figs. 6, 7, and 8). However, this bias may not necessarily always occur for other species showing a heartwood–sapwood colour change, which could be removed through traditional resin extraction methods. For the first time since the original concept papers by Björklund et al. (2014, 2015), we have experimented with the DB variable. The resulting reconstruction agrees well with a previous RW-based reconstruction (Wiles et al., 2014) and the glacial advance record (Wiles et al., 2004; Solomina et al., 2016) for the region.

The analyses presented herein must be viewed as a series of experiments to inform dendroclimatologists of possible methodological strategies that need to be considered for improving TR-based reconstructions using BI-based variables. Specific to the GOA region, but likely relevant to other regions and species, we therefore detail the following recommendations:

– Although MXD typically has a higher expressed population signal strength and climate responses than RW

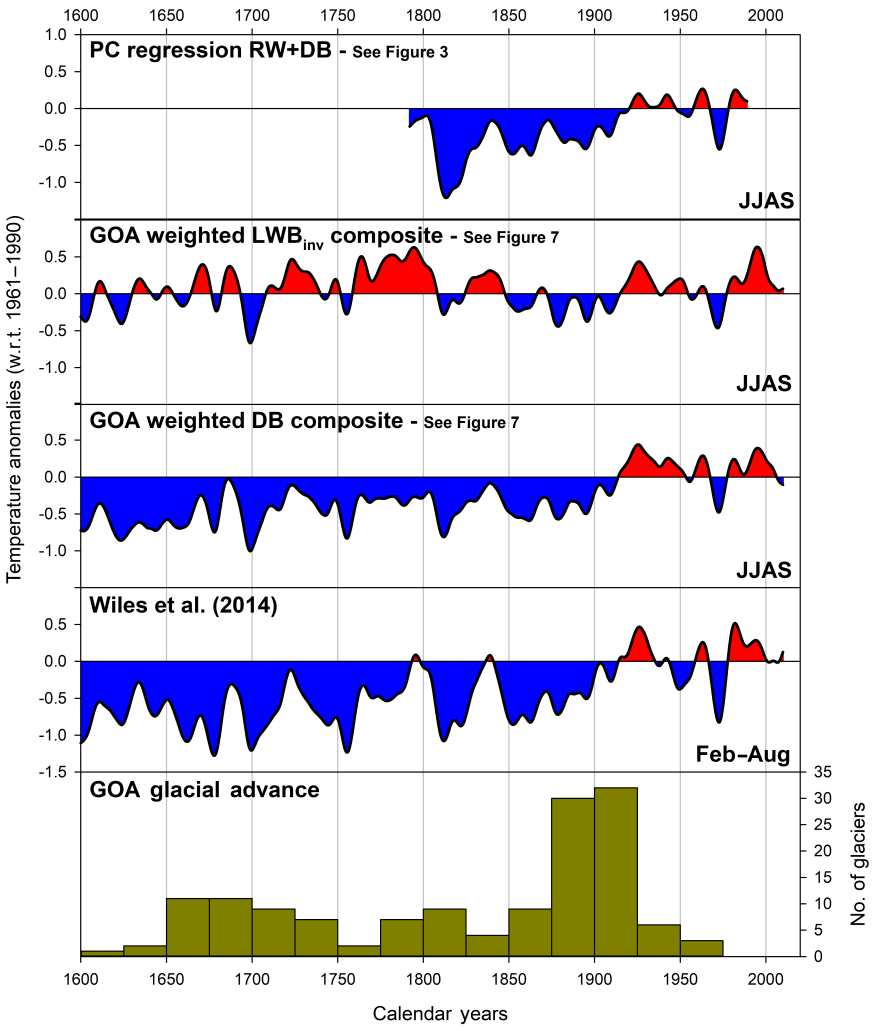

Figure 8. Comparison of GOA reconstruction variants using DB and RW with Wiles et al. (2014). The lower panel presents a histogram of glacial advance in the GOA region (Wiles et al., 2004; Solomina et al., 2016).

(Wilson and Luckman, 2003), signal strength in LWB and DB in GOA hemlock is weaker than RW; thus, replication needs to be substantially increased (ideally >20 trees, Table 1) to allow the development of robust chronologies. Rydval et al. (2014) also showed that a substantial improvement in LWB signal strength could be gained by measuring two or even three radii per tree. Additional assessments of signal strength should be conducted as new species and sites are analysed using BI methods.

– For conifer species with a clear colour difference between the heartwood and sapwood, LWB_{inv} may likely always contain biased long-term trends. The DB variable could potentially minimize this effect as shown here, but more experimentation with this parameter is needed before it can be commonly used as a solution to the LWB_{inv} colour bias problem. Rydval et al. (2017), using Scots pine, overcame the heartwood–sapwood colour bias by utilizing a band-pass approach to calibration, in which LWB_{inv} drove the decadal and high-frequency fraction of the Scottish temperature reconstruction, while RW drove the low-frequency variability. This approach however assumes that (1) RW is predominantly controlled by summer temperatures and (2) meaningful long-term information can be gleaned from RW data, which may not always be the case (Esper et al., 2012).

– There is substantial sensitivity of the final chronologies to varying methodological detrending approaches. Much more exploration of the impact of different detrending choices is needed and it is likely that ensemble-based approaches (Wilson et al., 2014) will ultimately be the only way to derive realistic estimates and appropriate detrending-based uncertainty bounds. Locations

with long instrumental records may help identify more optimal detrending options but care is needed, as it cannot be assumed that the quality of 19th century data is comparable to late 20th–early 21st century data. Utilizing other proxy observations of past climate (e.g. in this case the glacial record) may help further constrain TR estimates of past climate, especially when different chronology variants (that validate well) portray quite different past temperature histories.

Data availability. The main author can be contacted if individuals would like to access the raw or reconstructed data so that we can provide clear caveats of the experimental and/or preliminary nature of the data detailed in this paper.

The Supplement related to this article is available online at https://doi.org/10.5194/cp-13-1007-2017-supplement.

Competing interests. The authors declare that they have no conflict of interest.

Acknowledgements. We gratefully acknowledge the National Science Foundation's Paleoclimatic Perspectives on Climatic Change (P2C2) grant nos. AGS 1159430, AGS 1502186, AGS 1502150, and PLR 15-04134. The detailed reviews from Milos Rydval and Jesper Björklund were very much appreciated. Lamont-Doherty Earth Observatory contribution no. 8121 is also acknowledged.

Edited by: Hans Linderholm
Reviewed by: Jesper Björklund and Milos Rydval

References

Anchukaitis, K. J., Breitenmoser, P., Briffa, K. R., Buchwal, A., Büntgen, U., Cook, E. R., D'arrigo, R. D., Esper, J., Evans, M. N., Frank, D., and Grudd, H.: Tree rings and volcanic cooling, Nat. Geosci., 5, 836–837, 2012.

Anchukaitis, K. J., D'Arrigo, R. D., Andreu-Hayles, L., Frank, D., Verstege, A., Curtis, A., Buckley, B. M., Jacoby, G. C., and Cook, E. R.: Tree-ring-reconstructed summer temperatures from northwestern North America during the last nine centuries, J. Climate, 26, 3001–3012, 2013.

Anchukaitis, K. J., Wilson, R., Briffa, K., Büntgen, U., Cook, E. R., D'Arrigo, R., Davi, N., Esper, J., Frank, D., Gunnarson, B., Hegerl, G., Helama, S., Klesse, S., Krusic, P. J., Linderholm, H., Myglan, V., Osborn, T., Peng, Z., Rydval, M., Schneider, L., Schurer, A., Wiles, G., and Zorita, E.: Last millennium Northern Hemisphere summer temperatures from tree rings: Part II: spatially resolved reconstructions, Quaternary Sci. Rev., 163, 1–22, https://doi.org/10.1016/j.quascirev.2017.02.020, 2017.

Andreu-Hayles, L., D'Arrigo, R., Anchukaitis, K. J., Beck, P. S., Frank, D., and Goetz, S.: Varying boreal forest response to Arctic environmental change at the Firth River, Alaska, Environ. Res. Lett., 6, 045503, https://doi.org/10.1088/1748-9326/6/4/045503, 2011.

Barclay, D. J., Wiles, G. C., and Calkin, P. E.: A 1119-year tree-ring-width chronology from western Prince William Sound, southern Alaska, The Holocene, 9, 79–84, 1999.

Björklund, J., Gunnarson, B. E., Seftigen, K., Zhang, P., and Linderholm, H. W.: Using adjusted Blue Intensity data to attain high-quality summer temperature information: A case study from Central Scandinavia, The Holocene, 25, 547–556, 2015.

Björklund, J. A., Gunnarson, B. E., Seftigen, K., Esper, J., and Linderholm, H. W.: Blue intensity and density from northern Fennoscandian tree rings, exploring the potential to improve summer temperature reconstructions with earlywood information, Clim. Past, 10, 877–885, https://doi.org/10.5194/cp-10-877-2014, 2014.

Briffa, K. R. and Melvin, T. M.: A closer look at regional curve standardization of tree-ring records: justification of the need, a warning of some pitfalls, and suggested improvements in its application, in: Dendroclimatology, Springer Netherlands, 113–145, 2011.

Briffa, K. R., Jones, P. D., Schweingruber, F. H., Karlén, W., and Shiyatov, S. G.: Tree-ring variables as proxy-climate indicators: problems with low-frequency signals. In Climatic variations and forcing mechanisms of the last 2000 years, Springer, Berlin Heidelberg, Germany, 9–41, 1996.

Briffa, K. R., Osborn, T. J., Schweingruber, F. H., Jones, P. D., Shiyatov, S. G., and Vaganov, E. A.: Tree-ring width and density data around the Northern Hemisphere: Part 1, local and regional climate signals, The Holocene, 12, 737–757, 2002.

Campbell, R., McCarroll, D., Loader, N. J., Grudd, H., Robertson, I., and Jalkanen, R.: Blue intensity in Pinus sylvestris tree-rings: developing a new palaeoclimate proxy, The Holocene, 17, 821, https://doi.org/10.1177/0959683607080523, 2007.

Cook, E. R. and Peters, K.: The smoothing spline: a new approach to standardising forest interior tree-ring width series for dendroclimatic studies, Tree-Ring Bull., 41, 45–54, 1981.

Cook, E. R. and Peters, K.: Calculating unbiased tree-ring indices for the study of climatic and environmental change, The Holocene, 7, 361–370, 1997.

Cook, E. R., Briffa, K. R., and Jones, P. D.: Spatial regression methods in dendroclimatology: a review and comparison of two techniques, Int. J. Climatol., 14, 379–402, https://doi.org/10.1002/joc.3370140404, 1994.

Cowtan, K. and Way, R. G.: Coverage bias in the HadCRUT4 temperature series and its impact on recent temperature trends, Q. J. Roy. Meteor. Soc., 140, 1935–1944, 2014.

D'Arrigo, R., Villalba, R., and Wiles, G.: Tree-ring estimates of Pacific decadal climate variability, Clim. Dynam., 18, 219–224, 2001.

D'Arrigo, R., Wilson, R., Liepert, B., and Cherubini, P.: On the "divergence problem" in northern forests: a review of the tree-ring evidence and possible causes, Global Planet. Change, 60, 289–305, 2008.

Dolgova, E.: June–September temperature reconstruction in the Northern Caucasus based on blue intensity data, Dendrochronologia, 39, 17–23, 2016.

Ebbesmeyer, C. C., Cayan, D. R., McLain, D. R., Nichols, F. H., Peterson, D. H., and Redmond, K. T.: 1976 step in the Pacific climate: Forty environmental changes between 1968–75 and 1977–1984, in: Seventh Annual Pacific Climate (PACLIM) Workshop, 10–13 April 1990, Asilomar Conference Center, Pacific Grove, CA, USA, 115–126, 1991.

Esper, J., Cook, E. R., Peters, K., and Schweingruber, F. H.: Detecting low frequency tree-ring trends by the RCS method, Tree-Ring Res., 59, 81–98, 2003.

Esper, J., Frank, D. C., Wilson, R. J., and Briffa, K. R.: Effect of scaling and regression on reconstructed temperature amplitude for the past millennium, Geophys. Res. Lett., 32, L07711, https://doi.org/10.1029/2004GL021236, 2005.

Esper, J., Frank, D. C., Timonen, M., Zorita, E., Wilson, R. J., Luterbacher, J., Holzkämper, S., Fischer, N., Wagner, S., Nievergelt, D., and Verstege, A.: Orbital forcing of tree-ring data, Nature Climate Change, 2, 862–866, 2012.

Esper, J., Schneider, L., Smerdon, J. E., Schöne, B. R., and Büntgen, U.: Signals and memory in tree-ring width and density data, Dendrochronologia, 35, 62–70, 2015.

Frank, D., Esper, J., and Cook, E. R.: Adjustment for proxy number and coherence in a large-scale temperature reconstruction, Geophys. Res. Lett., 34, L16709, https://doi.org/10.1029/2007GL030571, 2007a.

Frank, D., Büntgen, U., Böhm, R., Maugeri, M., and Esper, J.: Warmer early instrumental measurements versus colder reconstructed temperatures: shooting at a moving target, Quaternary Sci. Rev., 26, 3298–3310, 2007b.

Harris, I. P. D. J., Jones, P. D., Osborn, T. J., and Lister, D. H.: Updated high-resolution grids of monthly climatic observations – the CRU TS3. 10 Dataset, Int. J. Climatol., 34, 623–642, 2014.

Luckman, B. H. and Wilson, R. J. S.: Summer temperatures in the Canadian Rockies during the last millennium: a revised record, Clim. Dynam., 24, 131–144, 2005.

Mantua, N. J., Hare, S. R., Zhang, Y., Wallace, J. M., and Francis, R. C.: A Pacific interdecadal climate oscillation with impacts on salmon production, B. Am. Meteorol. Soc., 78, 1069–1079, 1997.

McCarroll, D., Pettigrew, E., Luckman, A., Guibal, F., and Edouard, J. L.: Blue reflectance provides a surrogate for latewood density of high-latitude pine tree rings, Arct. Antarct. Alp. Res., 34, 450–453, 2002.

Melvin, T. M. and Briffa, K. R.: A "signal-free" approach to dendroclimatic standardisation, Dendrochronologia, 26, 71–86, 2008.

Melvin, T. M. and Briffa, K. R.: CRUST: Software for the implementation of Regional Chronology Standardisation: Part 2. Further RCS options and recommendations, Dendrochronologia, 32, 343–356, 2014.

Melvin, T. M., Briffa, K. R., Nicolussi, K., and Grabner, M.: Time-varying-response smoothing, Dendrochronologia, 25, 65–69, 2007.

Morice, C. P., Kennedy, J. J., Rayner, N. A., and Jones, P. D.: Quantifying uncertainties in global and regional temperature change using an ensemble of observational estimates: The HadCRUT4 data set, J. Geophys. Res.-Atmos., 117, https://doi.org/10.1029/2011JD017187, 2012.

Rohde, R., Muller, R. A., Jacobsen, R., Muller, E., Perlmutter, S., Rosenfeld, A., Wurtele, J., Groom, D., and Wickham, C.: A new estimate of the average Earth surface land temperature spanning 1753 to 2011, Geoinfor. Geostat., 1, 1–7, 2012.

Rydval, M., Larsson, L. Å., McGlynn, L., Gunnarson, B. E., Loader, N. J., Young, G. H., and Wilson, R.: Blue intensity for dendroclimatology: should we have the blues? Experiments from Scotland, Dendrochronologia, 32, 191–204, 2014.

Rydval, M., Druckenbrod, D., Anchukaitis, K. J., and Wilson, R.: Detection and removal of disturbance trends in tree-ring series for dendroclimatology, Can. J. Forest Res., 46, 387–401, 2015.

Rydval, M., Loader, N. J., Gunnarson, B. E., Druckenbrod, D. L., Linderholm, H. W., Moreton, S. G., Wood, C. V., and Wilson, R.: Reconstructing 800 years of summer temperatures in Scotland from tree rings, Clim. Dynam., 1–24, https://doi.org/10.1007/s00382-016-3478-8, online first, 2017.

Schneider, L., Smerdon, J. E., Büntgen, U., Wilson, R. J., Myglan, V. S., Kirdyanov, A. V., and Esper, J.: Revising midlatitude summer temperatures back to AD 600 based on a wood density network, Geophys. Res. Lett., 42, 4556–4562, 2015.

Schweingruber, F.: Tree Rings: Basics and Applications of Dendrochronology, Springer, NY, USA, 1988.

Solomina, O. N., Bradley, R. S., Jomelli, V., Geirsdottir, A., Kaufman, D. S., Koch, J., McKay, N. P., Masiokas, M., Miller, G., Nesje, A., and Nicolussi, K.: Glacier fluctuations during the past 2000 years, Quaternary Sci. Rev., 149, 61–90, 2016.

Wigley, T. M., Briffa, K. R., and Jones, P. D.: On the average value of correlated time series, with applications in dendroclimatology and hydrometeorology, J. Clim. Appl. Meteorol., 23, 201–213, 1984.

Wiles, G. C., D'Arrigo, R. D., Villalba, R., Calkin, P. E., and Barclay, D. J.: Century-scale solar variability and Alaskan temperature change over the past millennium, Geophys. Res. Lett., 31, L15203, https://doi.org/10.1029/2004GL020050, 2004.

Wiles, G. C., D'Arrigo, R. D., Barclay, D., Wilson, R. S., Jarvis, S. K., Vargo, L., and Frank, D.: Surface air temperature variability reconstructed with tree rings for the Gulf of Alaska over the past 1200 years, The Holocene, 24, 198–208, 2014.

Wilson, R., Wiles, G., D'Arrigo, R., and Zweck, C.: Cycles and shifts: 1300 years of multi-decadal temperature variability in the Gulf of Alaska, Clim. Dynam., 28, 425–440, https://doi.org/10.1007/s00382-006-0194-9, 2007.

Wilson, R., Rao, R., Rydval, M., Wood, C., Larsson, L. Å., and Luckman, B. H.: Blue Intensity for dendroclimatology: The BC blues: A case study from British Columbia, Canada, The Holocene, 24, 1428–1438, 2014.

Wilson, R., Anchukaitis, K., Briffa, K., Büntgen, U., Cook, E., D'Arrigo, R., Davi, N., Esper, J., Frank, D., Gunnarson, B., Hegerl, G., Klesse, S., Krusic, P., Linderholm, H., Myglan, V., Peng, Z., Rydval, M., Schneider, L., Schurer, A., Wiles, G., and Zorita, E.: Last millennium northern hemisphere summer temperatures from tree rings: Part I: The long term context, Quaternary Sci. Rev., 134, 1–18, 2016.

Wilson, R., Wilson, D., Rydval, M., Crone, A., Büntgen, U., Clark, S., Ehmer, J., Forbes, E., Fuentes, M., Gunnarson, B. E., and Linderholm, H. W.: Facilitating tree-ring dating of historic conifer timbers using Blue Intensity, J. Archaeol. Sci., 78, 99–111, 2017.

Wilson, R. J. and Luckman, B. H.: Dendroclimatic reconstruction of maximum summer temperatures from upper treeline sites in Interior British Columbia, Canada, The Holocene, 13, 851–861, 2003.